Active, Adjustable Audio Band-Pass Filter*

J. Ross Macdonald
Texas Instruments, 6000 Lemmon Avenue, Dallas 9, Texas
(Received August 19, 1957)

An active, adjustable band-pass filter having seventh-order Butterworth attenuation characteristics (42 db/octave slopes) is described. It has 34 separate high-pass cutoff frequencies between 16.2 cps and 16 200 cps and 34 low-pass cutoffs between 20 cps and 20 000 cps. The filter weighs six pounds exclusive of power supply and uses six miniature double triodes and no inductors. Its insertion gain is 4.5 db, its dynamic range exceeds 110 db, and it will supply more than 50 v rms output with low distortion. Second-order harmonic distortion is much reduced by running tube heaters at about 3.7 v, leading to greatly increased tube life. Intermodulation distortion at 10 v rms output is only 0.065%.

I. INTRODUCTION

THERE are many applications for a small, adjustable audio band-pass filter having sharp cutoff characteristics. The filter to be described is adaptable for sound analysis[1] and can be designed with fractional octave steps for such an application. Its very sharp cutoff slopes, wide dynamic range, and low noise make it particularly valuable for a variety of measurements in the audio field.

By making the filter active, all inductances could be eliminated, with consequent reduction of size, weight, distortion, hum pickup, and extension of the dynamic range. In the interest of obtaining sharp corners and high cutoff slopes with a minimum of complication, it was decided to design both high-pass and low-pass sections of the filter to achieve seventh-order Butterworth characteristics, giving cutoff slopes of 42 db/octave.

In a seventh-order filter of the type considered, seven elements must be simultaneously varied in order to alter the cutoff frequency. Because of the difficulty of achieving accurate tracking of seven ganged elements, it was decided to change the cutoff frequency by switching the elements in discrete steps. Each decade was divided into eleven intervals, equally spaced on a logarithmic frequency scale. Thus, the ratio between two successive cutoff frequencies is $10^{1/11}=1.23285$. The selected frequencies and ideal cutoff characteristics are shown in Fig. 1. There are 34 separate high-pass cutoffs from 16.2 cps to 16 200 cps and 34 low-pass cutoffs running from 20 cps to 20 000 cps. In the succeeding sections, we shall discuss the circuits which yield these characteristics and the results of measurements of the filter capabilities.

II. CIRCUIT DESIGN

The absolute value of the input-output voltage transfer ratio, $S(i\omega)$, of a seventh order, low-pass Butterworth filter having unity transfer ratio in the pass region may be written as $|S(i\omega)|=[1+\omega^{14}]^{-\frac{1}{2}}$, where the cutoff radial frequency ω_0 has been normalized to unity for convenience. To design a circuit to realize such response, it is desirable to have available the expression for $S(i\omega)$ itself or, preferably, that for $S(p)$, where p is a complex frequency variable, $p=\sigma+i\omega$, and σ is a small constant. A method for deriving $S(p)$ from $|S(i\omega)|$ is outlined in Appendix I, yielding for the present case

$$S(p)=[(p+1)(p^2+d_1p+1)\times(p^2+d_2p+1)(p^2+d_3p+1)]^{-1},$$

where

$$d_m=2\cos(\pi m/7),\quad m=1, 2, 3.$$

The foregoing expression for $S(p)$ shows that the poles of the transfer function lie on a unit-radius semicircle with center at $p=0$ in the left half of the complex p plane. There is a pole at $p=-1$ and conjugate poles on the semicircle at $\phi=\pm m\pi/7$, $m=1, 2, 3$. The pole diagram for the high-pass case is similar except that there is a seventh-order zero at the origin in addition.

Sallen and Key[2] have shown how Butterworth response of any order can be realized with a chain of simple active feedback circuits. The elemental circuits are shown in Fig. 2 together with their ideal responses. In Fig. 3, these elements are shown connected together in block diagram form to give seventh-order low-pass and high-pass sections. Cathode followers are used to give those K values shown less than unity in Fig. 2, while augmented cathode followers[3] (ACF) are used for K's greater than unity. These circuits also supply the necessary buffering between the various elemental frequency selective circuits.

Let us define $T_1=R_1C_1$, $T_2=R_2C_2$, $\rho=R_1/R_2$, and $\gamma=C_2/C_1$. Then in the low-pass case, the following

* This paper was presented in part at the Ninth Southwestern Institute of Radio Engineers Conference, Houston, Texas (April 12, 1957).

[1] H. H. Scott and D. Von Recklinghausen, J. Acoust. Soc. Am. 25, 727–731 (1953).

[2] R. P. Sallen and E. L. Key, Trans. Inst. Radio Engrs. CT-2, 74–85 (1955). Also, MIT Lincoln Laboratory Technical Report No. 50 (May 6, 1954); a more complete treatment.

[3] J. R. Macdonald, Trans. Inst. Radio Engrs. AU-5, 63–70 (1957).

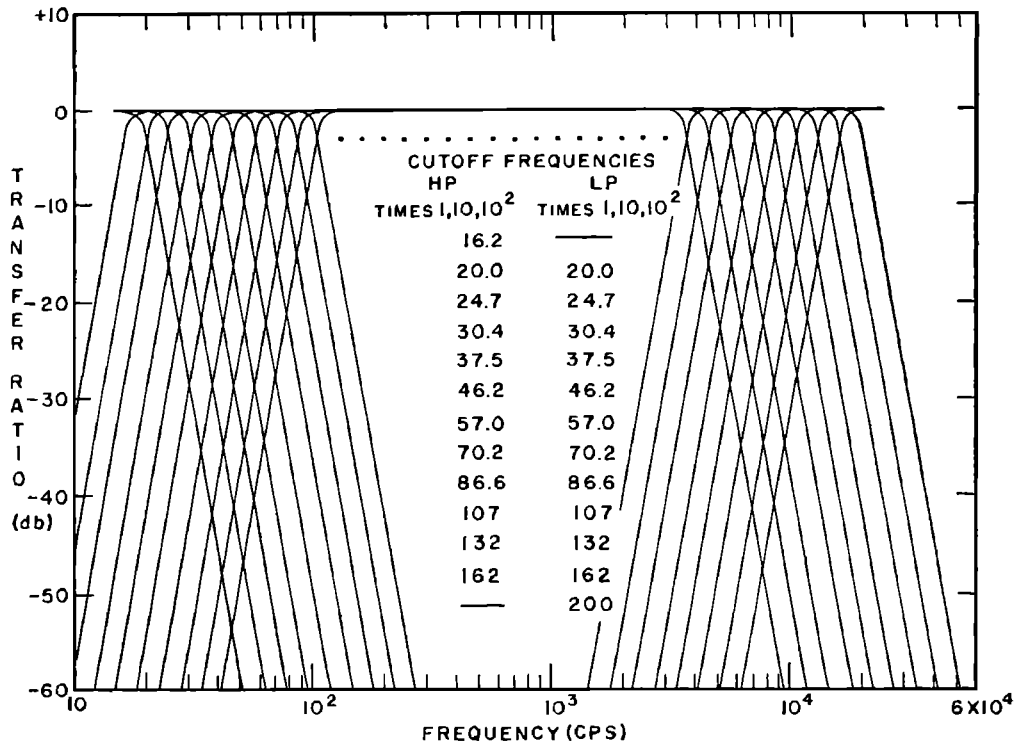

FIG. 1. High-pass and low-pass cutoff frequencies and ideal slopes.

equations given by Sallen and Key are available for the calculation of element values

$$T_2=\frac{d}{2(1+\rho)}\left[1\pm\left\{1-\frac{4(1+\rho)(1-K)}{d^2}\right\}^{\frac{1}{2}}\right], \quad (1)$$

$$=\frac{d}{2}\left[1\pm\left\{1-\frac{4(1+\gamma-K)}{d^2}\right\}^{\frac{1}{2}}\right], \quad (2)$$

$$T_1=\frac{d}{2(1-K)}\left[1\pm\left\{1-\frac{4(1+\rho)(1-K)}{d^2}\right\}^{\frac{1}{2}}\right], \quad (3)$$

$$=\frac{d}{2(1+\gamma-K)}\left[1\pm\left\{1-\frac{4(1+\gamma-K)}{d^2}\right\}^{\frac{1}{2}}\right], \quad (4)$$

$$T_1T_2=1. \quad (5)$$

For the high-pass case, the same equations apply after the following transformations: $\rho\rightarrow\gamma$, $\gamma\rightarrow\rho$, $T_1\rightarrow T_2$, $T_2\rightarrow T_1$. These equations are given for a cutoff radial frequency $\omega_0=1$. Note that when $K=1$, Eq. (3) yields $T_1=(1+\rho)/d$.

The foregoing equations are applied, for a given value of d, by making a choice of K and γ or ρ, then calculating T_1 and T_2. Since the element values depend on K, it is important that it be stable; the cathode followers and augmented cathode followers used in the present design satisfy this requirement well. After T_1 and T_2 have been obtained, the relation $T_1\gamma=T_2\rho$ can be used to determine whichever of γ or ρ was not initially chosen. For most cases, the formulas yield two possible values for each of the T's. Sallen and Key point out that it will be generally preferable to select the value of T which minimizes the dependence of d on K so that the characteristics of the filter are least dependent on the voltage amplification of the active elements.

After d, K, ρ, γ, T_1, and T_2 have been selected and calculated, the selection of a specific value for any one of the resistances or capacitances fully determines the others for a value of ω_0 of unity. For any other ω_0, all capacitances or all resistances are simply divided by ω_0 to yield the values appropriate for that cutoff frequency. The determination of the simple transfer circuits involving R_0 and C_0 follows from the relation $1=\omega_0R_0C_0$ and a specific choice for one of these elements.

III. CIRCUIT DETAILS

It was decided to obtain the twelve cutoff frequencies within each frequency decade by switching resistor values, and to achieve frequency multiplication factors of 10 and 100 by switching capacitors. On applying the principles and equations of the last section, the element values shown in Tables I to III were derived. All resistance values are in kilohms and all capacitance values in microfarads. The capacitances shown in Table III apply to the lowest frequency decade; values smaller by 10 and 100 times apply for the two higher decades.

In building the filter, frequency-determining capaci-

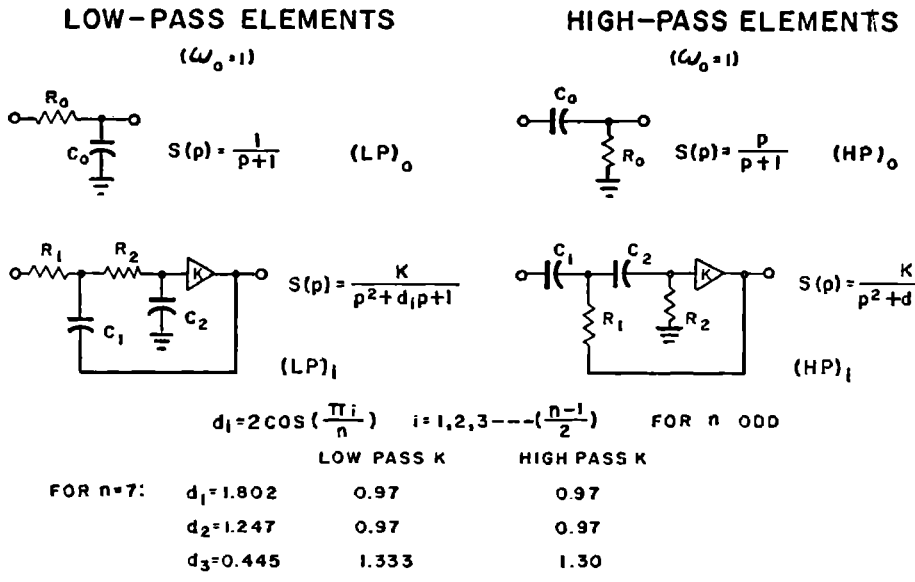

FIG. 2. Elemental frequency-determining circuits.

$$d_i = 2\cos\left(\frac{\pi i}{n}\right) \quad i = 1,2,3---\left(\frac{n-1}{2}\right) \quad \text{FOR } n \text{ ODD}$$

		LOW PASS K	HIGH PASS K
FOR n=7:	d_1=1.802	0.97	0.97
	d_2=1.247	0.97	0.97
	d_3=0.445	1.333	1.30

tors were selected to within about one percent of their nominal values. The 168 frequency-determining resistors were selected from five-percent-tolerance units to within two to three percent of nominal. Figure 4 shows the circuit of the filter with switches for changing resistor and capacitor values omitted. The switches shown allow the low-pass and the high-pass sections to be used in series, either section separately, or neither section. It will be noted that the low-pass section is

TABLE I. Low-pass frequency-determining resistor values ($K\Omega$).

f_0 (cps)	R_0	d=1.802 R_1	d=1.802 R_2	d=1.247 R_1	d=1.247 R_2	d=0.445 R_1	d=0.445 R_2
20.00	795.82	944.48	446.98	571.73	369.21	596.14	354.15
24.66	645.43	766.00	362.52	463.69	299.44	483.49	287.22
30.40	523.56	621.37	294.07	376.14	242.90	392.20	232.99
37.48	424.66	503.99	238.52	305.09	197.02	318.11	188.98
46.20	344.51	408.87	193.50	247.50	159.83	258.07	153.31
56.96	279.43	331.63	156.95	200.75	129.64	209.32	124.35
70.23	226.63	268.97	127.29	162.82	105.14	169.77	100.85
86.58	183.83	218.17	103.25	132.07	85.29	137.71	81.81
106.74	149.11	176.97	83.75	107.13	69.18	111.70	66.36
131.59	120.93	143.55	67.94	86.90	56.12	90.60	53.83
162.23	98.11	116.44	55.10	70.48	45.52	73.49	43.66
200.00	79.58	94.45	44.70	57.17	36.92	59.61	35.42

TABLE II. High-pass frequency-determining resistor values ($K\Omega$).

f_0 (cps)	R_0	d=1.802 R_1	d=1.802 R_2	d=1.247 R_1	d=1.247 R_2	d=0.445 R_1	d=0.445 R_2
16.22	981.1	867.3	1109.8	587.1	1639.3	325.3	976.0
20.00	795.82	703.51	900.21	476.23	1329.7	263.87	791.68
24.66	645.43	570.57	730.10	386.23	1078.4	214.00	642.08
30.40	523.56	462.84	592.24	313.31	874.81	173.60	520.84
37.48	424.66	375.41	480.37	254.12	709.56	140.80	422.46
46.20	344.51	304.55	389.70	206.16	575.64	114.23	342.72
56.96	279.43	247.02	316.09	167.21	466.90	92.65	277.98
70.23	226.63	200.35	256.36	135.62	378.68	75.14	225.46
86.58	183.83	187.38	207.95	110.01	307.17	60.95	182.88
106.74	149.11	131.82	168.67	89.23	249.15	49.44	148.34
131.59	120.95	106.92	136.82	72.38	202.10	40.10	120.33
162.23	98.11	86.73	110.98	58.71	163.93	32.53	97.60

TABLE III. Active-element transfer ratios, K, and frequency-determining capacitors (microfarads) for the lowest decade.

d	K LP	K HP	C_0 LP	C_0 HP	C_1 LP	C_1 HP	C_2 LP	C_2 HP
···	0.97	0.97	0.01	0.01	···	···	···	···
1.802	0.97	0.97	···	···	0.015	0.01	0.01	0.01
1.247	0.97	0.97	···	···	0.03	0.01	0.01	0.01
0.445	1.333	1.300	···	···	0.03	0.01	0.01	0.03

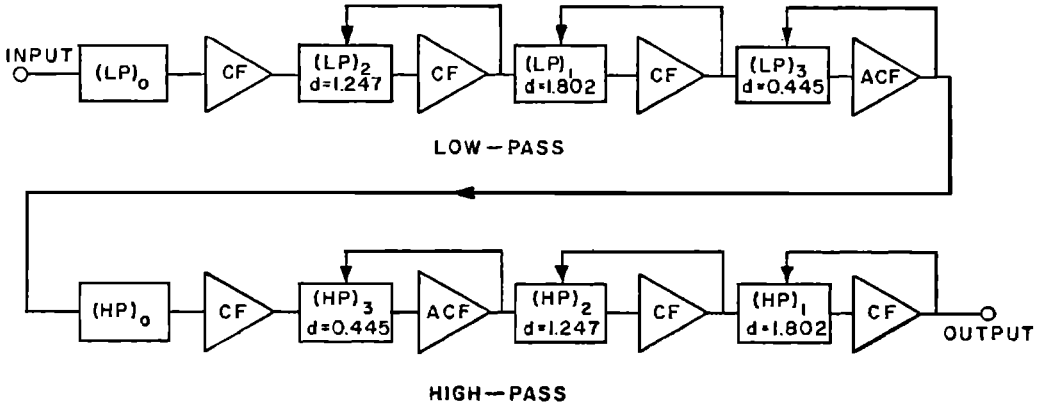

FIG. 3. Block diagram of filter sections.

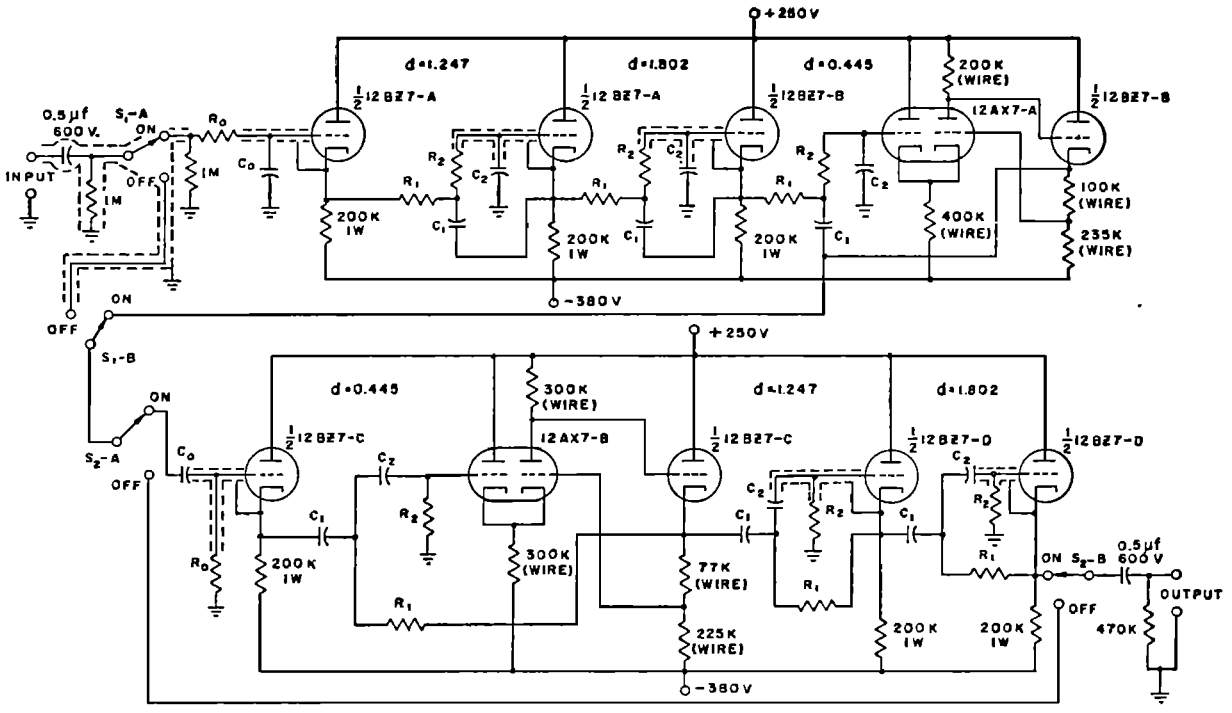

FIG. 4. Filter circuit with switching of frequency-determining elements omitted.

entirely direct coupled and could be employed separately where a direct-coupled filter was desirable.

The 12BZ7 cathode followers used were found to be superior to 12AT7's in having an input-output voltage transfer ratio, K, nearer unity and a lower output impedance. The factor K varied from 0.98 with an added output load of 115 kilohms to 0.96 with an added load of 15 kilohms. Since switching of the frequency-determining resistors puts a varying load on the cathode-follower circuits, it is desirable to pick the impedance level such that the change from minimum to maximum load alters K as little as possible. On the other hand, with too high an impedance level, the effect of stray capacitances will become important at the higher frequencies. The impedance level has been selected so that all cathode-follower K's lie between about 0.982 and 0.97. The latter figure has been used in all the calculations, and the actual small variations of K with load have been found to exert negligible effect on the filter characteristics.

The circuit uses two augmented cathode followers. Their output impedance is so low that variable loading has no measurable effect on their K values. Values of K greater than unity are achieved here by tapping down the feedback line on the output cathode resistor. Distortion is very low in the ACF circuits and, like cathode followers, they produce no phase inversion.

It will be noted that in the cathode follower circuits, the input shields are driven by the output. Since the output is in phase with and almost equal to the input, this technique reduces the effect of stray capacity to ground and of capacity between shield and input very appreciably. The minimum input resistance of the filter is about 80 kilohms. It could be made much greater by using a separate input isolation stage. The output resistance is about 350 ohms. By placing an ACF last, it could be reduced to about 5 ohms; it was felt more desirable, however, to use the low ACF output resistance to drive frequency-selective elements instead of the output.

Figures 5 and 6 show two views of the filter exclusive of power supply. It weighs six pounds, and it will be noted that the six vacuum tubes are located on an internal shock-mounted plate. Lettering is inscribed directly on the front panel of polished aluminum which is protected by a transparent plastic plate. A momen-

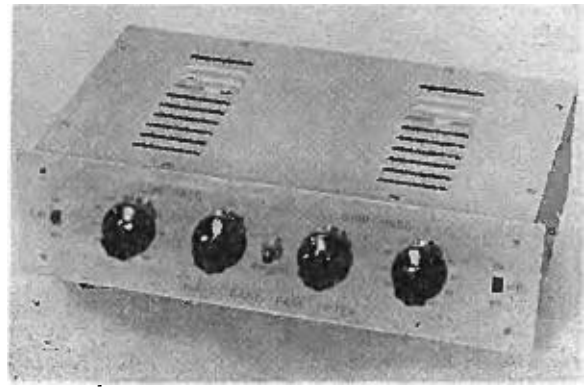

FIG. 5. View of filter from the front.

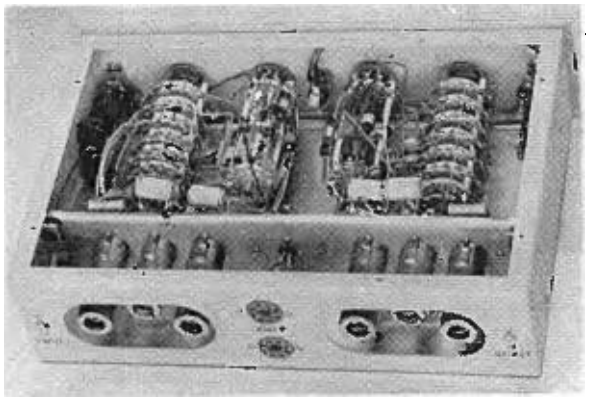

FIG. 6. View of inside of filter from the back.

tary-off switch (not shown in the circuit diagram) is located in the center of the front panel and is useful for eliminating switching transients during very low level work. Both the front and back side panels are removable. The instrument draws 16 ma from the high voltage supplies and requires about 9 w of heater power.

IV. PERFORMANCE

Before measuring the performance in detail, the two ACF K values were adjusted to give the closest approximation to maximally flat or Butterworth response in the neighborhood of all of the cutoff frequencies. In spite of selecting the many resistance values to only two or three percent tolerance, it was found that all cutoff regions approximated ideal Butterworth response to within ± 1 db and that many were much closer than that to ideal. Only when several of the resistance tolerances were off in the same direction did as much as a 1-db deviation above or below ideal response occur. In the majority of the cases, resistance deviations in opposite directions canceled out.

The input-output voltage transfer ratio of the low-pass section was found to be 1.33 while that of the high-pass section was 1.26, making the voltage amplification ratio of both sections in series 1.68, or 4.5 "db." These results apply for all positions of the low-pass section but are slightly altered for the $f\times 100$ position of the high-pass section. There, the high-pass voltage transfer ratio is reduced by 4 db compared to the $f\times 1$ and $f\times 10$ positions. This reduction is independent of cutoff position (resistance values) and arises from unavoidable stray capacitance to ground. The effect could have been reduced or eliminated entirely by making all high-pass capacitance values ten times larger and all resistance values ten times smaller. This reduction in impedance level would have caused appreciable change in cathode follower K's with cutoff position, however, because of the increased loading and would have necessitated replacement of these cathode followers by ACF's if no change of high-pass voltage transfer ratio and corner shape with cutoff position were required. The impedance level is similarly high in the low-pass section, but voltage amplification reduction in the $f\times 100$ position can be eliminated since the important stray capacitance is there in parallel with the frequency-determining capacitances. By using variable trimmer capacitances in the $f\times 100$ position, the values of all C_0, C_1, and C_2 capacitances can be set once and for all to their correct values, including stray capacitance effects, to yield Butterworth response.

Typical amplitude and phase characteristics for two different settings of the filter are shown in Fig. 7. Because of unavoidable harmonic distortion in the oscillator used, the high-pass amplitude characteristic with $f_{HP}=1070$ cps, $f_{LP}=20\,000$ cps had to be measured with a wave analyzer. The low-pass characteristic could be measured with either the wave analyzer or a wide-band ac voltmeter. Phase was measured using a Technology Instrument Corporation Type 320 A phasemeter. The intrinsic noise output of the filter set for maximum band pass ($f_{HP}=16$ cps, $f_{LP}=20\,000$ cps) was less than 100 μv rms measured with a voltmeter of wider band width.

The residual 6 db/octave slope in the low-pass characteristic of Fig. 7 arises from feedthrough. It is relatively independent of cutoff value within a decade but depends directly on the size of the capacitances in the low-pass section. In the $f\times 10$ position shown, this limiting slope begins at an attenuation of about 85 db. For the $f\times 100$ position it begins at about 65 db attenuation, and for the $f\times 1$ it appears at approximately 105 db attenuation provided the signal level still exceeds the noise level. These results suggest that if the impedance level in the low-pass section were reduced by making all frequency-determining capaci-

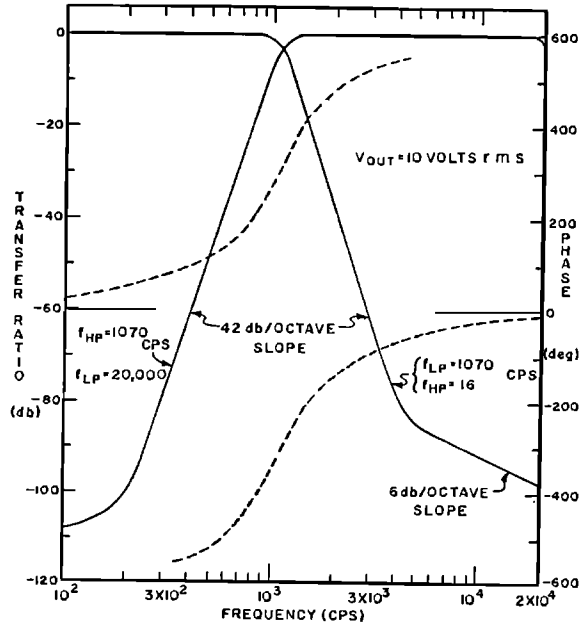

FIG. 7. Typical amplitude and phase characteristics.

tors larger and all resistors smaller by a factor of ten, one could achieve an appreciably increased region of attenuation of 42 db/octave slope in the $f\times100$ and $f\times10$ positions. For most practical purposes, however, the present attenuations are quite adequate.

The amplitude response curves of Fig. 7 are within better than 1 db of ideal Butterworth response over their entire regions until the final high-attenuation curvature sets in. Since the attenuation at cutoff should be 3 db, when both low-pass and high-pass sections are set to the same cutoff frequency the combined attenuation should be 6 db at the peak of the resulting inverted V characteristic. In the large majority of cases, the attenuation is 6 db ±1 db; in a few cases, the deviation may be as large as ±2 db. This is a stringent test of both the shapes of the attenuation curves near cutoff and the correspondence of the actual and calculated cutoff frequencies. Direct measurement shows that all cutoff frequencies agree within 3% with their calculated values and many are appreciably closer.

The upper dashed phase curve of Fig. 7 is associated with the low-pass amplitude curve. It approaches a high-frequency limiting value of 560 degrees, while the lower phase curve approaches a value of -560 degrees. These phase shifts are quite appreciable. J. Moir and others have shown,[4] however, that tremendous phase shifts are required to cause audible effects. For example, phase shifts of about 23 000 degrees at 8 kcps and 2500 degrees at 100 cps were found necessary. Using an all-pass phase-shifting network, Moir found that there was no audible difference between ordinary square waves and square waves whose harmonic components

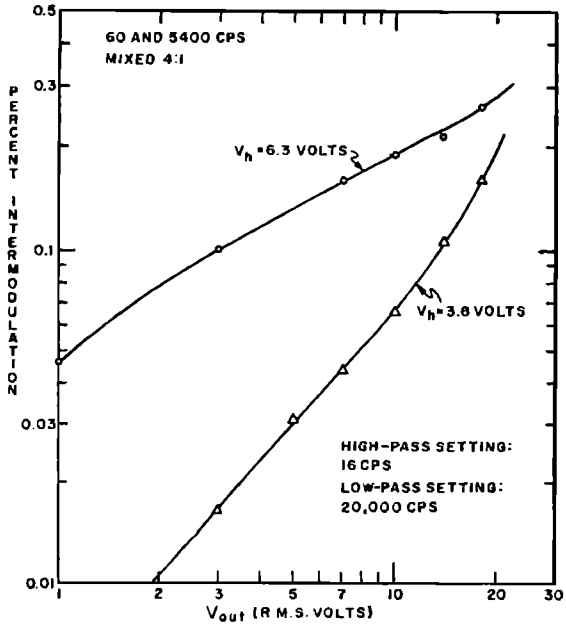

FIG. 8. Intermodulation distortion *versus* output voltage for two different heater voltages.

[4] J. Moir, Wireless World 62, 165–168 (1956).

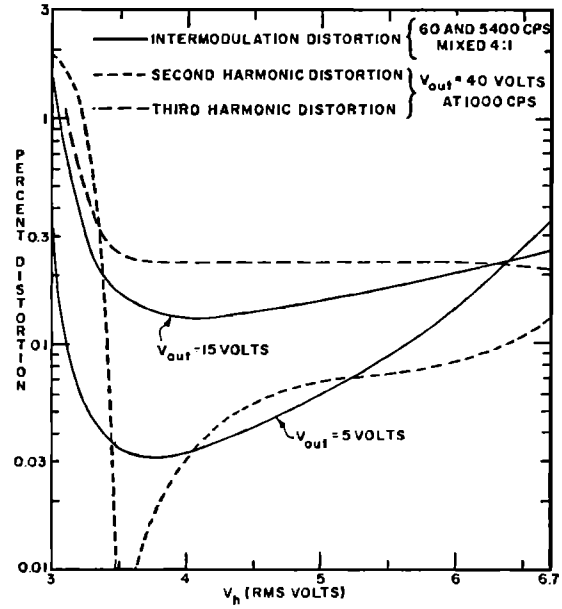

FIG. 9. Intermodulation and harmonic distortion *versus* heater voltage.

were so shifted in phase as to cause large peaking at the rise and fall points. We may thus conclude that the present phase shifts will not be of audible consequence.

It has already been mentioned that when f_{HP} and f_{LP} are set equal, the resulting characteristic is an inverted V with 42 db/octave side slopes. When the high and low-pass cutoffs are separated by one step, the top of the characteristic is more rounded and is about 1.2 db under the normal transmission of the filter. With two or more steps between high- and low-pass settings, the top of the band-pass characteristic is not reduced compared with the normal transmission, and it shows a definite flat portion with three or more steps of separation.

The dynamic range of the filter is very great. Because of the use of cathode followers and ACF circuits, it will handle an output of more than 50 v rms without appreciable distortion. The total dynamic range therefore exceeds 110 db. Having no inductors, the filter is not susceptible to hum pickup from magnetic fields.

Figure 8 shows the measured intermodulation distortion of the filter for two different heater voltages applied to all tubes. The distortion is naturally somewhat higher if any of the measuring frequencies are very close to cutoff. The interesting effect of heater voltage in reducing distortion is clarified in Fig. 9. It was difficult to measure the small harmonic distortion voltages for a fundamental output voltage much below 40 v rms. The measurements shown in Fig. 9 show, however, that the third harmonic distortion is virtually independent of heater voltage (or current) until such low voltages are reached that cathode

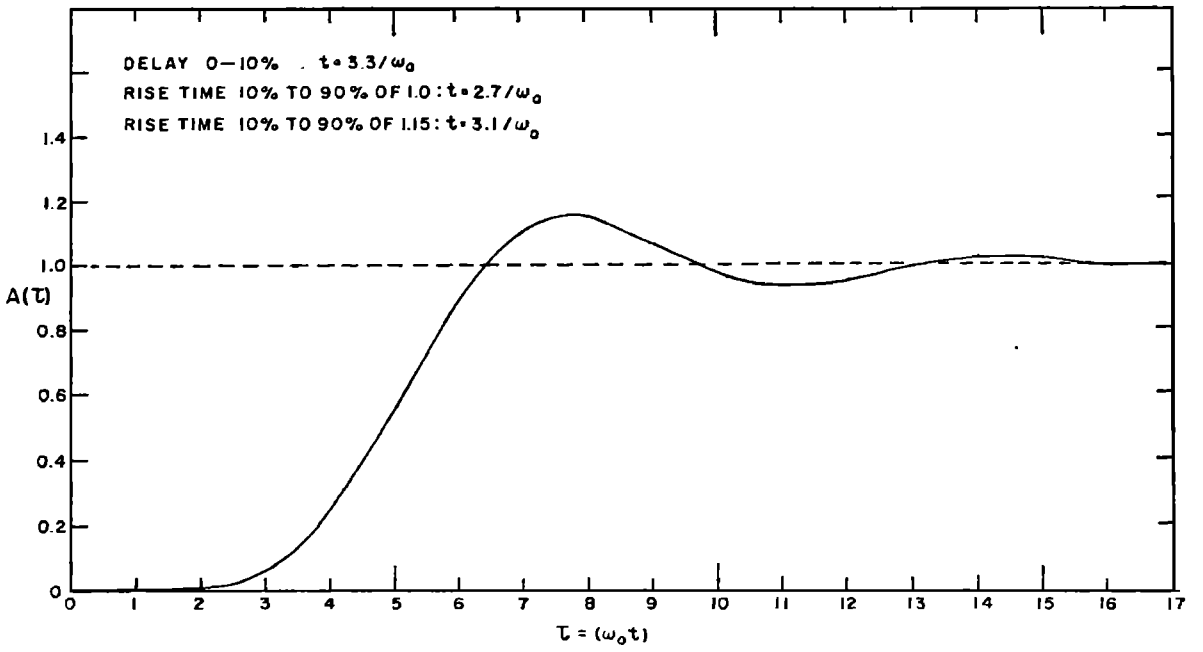

FIG. 10. Step-function response of low-pass, seventh-order Butterworth filter.

emission drops very rapidly. Similarly, the fundamental component is independent of heater-voltage until this level is reached. On the other hand, the second harmonic goes virtually to zero just before the point is reached where the emission drops quickly. Since the second harmonic is the major harmonic component at the lower output voltages, Figs. 8 and 9 show that the intermodulation distortion is also appreciably reduced at the lower outputs by reducing the heater voltage to the region where second-harmonic distortion is negligible. This conclusion is also borne out by the different slopes of the two curves of Fig. 8. It should be mentioned that the low distortion values shown in Figs. 8 and 9 are also contingent on proper selection of the positive and negative supply voltages.

Second-harmonic cancellation of the above form arises from a dependence of the input-output transfer characteristics of the various tubes of the filter on cathode temperature. At a certain temperature, the curvatures of these characteristics are apparently just right to yield a combined characteristic with no second-order harmonic-generating components over quite a wide dynamic range. Since the specifications of the filter are improved by operation with 3.5–3.8 v on the heaters, it is normally run in this condition. Besides reducing the required heater power by more than three times, this reduction in heater voltage very greatly extends the life of the heaters and cathodes of the tubes in the filter.

The transient response of the low-pass section of the filter, $A(t)$, for a unit step voltage input has been calculated and the method used is outlined in Appendix II. The result of the calculation is plotted in terms of the variable $\tau=\omega_0 t$ in Fig. 10. It will be noted that the filter exhibits an overshoot of about 15% and damped oscillation. Square-wave measurements on the present filter yield results which agree excellently with Fig. 10. The overshoot and damped oscillation are necessary concomitants of the sharp cutoff slope of the filter as long as it remains a minimum-phase device. This requirement might be relaxed by adding an all-pass section to the filter which could be designed to so reduce the phase shift in the region $0<f<3f_{LP}$ that negligible transient distortion would result. Due to the complexity of such a circuit, however, it is not practical in a small filter with a large number of cutoff frequencies. Corrington[5] has approached the problem by placing traps tuned to frequencies above cutoff in series with a low-pass filter. Although these traps can virtually eliminate overshoot and ringing, they also seem to reduce the attenuation slope past cutoff. In a filter with a number of cutoffs, their element values would have to be varied with cutoff frequency.

In the present filter, the use of trimmer capacitors in the $f\times100$ low-pass range allows the response of the filter to be easily altered for this range. When the capacitors are adjusted for perfect square-wave response, it is found, as expected, that the roll-off of the filter is much slower than the maximally-flat characteristic and that much more attenuation occurs in the region of cutoff. The results of Moir already cited on square-wave phase distortion suggest that the overshoot and ringing occurring with minimum phase Butterworth response will not lead to perceptible or at least appreciable audible consequences.

[5] M. S. Corrington, Proc. Natl. Elect. Conf. 10, 207–216 (1954).

APPENDIX I

Given the absolute value of the transfer ratio $|S(i\omega)|=[1+\omega^{14}]^{-\frac{1}{2}}$, we wish to derive the corresponding ratio itself written as a function of the complex frequency variable, p. We have

$$\begin{aligned}|S(i\omega)|^{-2}&=[S(p)S(p^*)]^{-1}=1+\omega^{14}\\&=(\omega^2+1)\prod_{m=1}^{3}(\omega^2-e^{i(2m-1)\theta})(\omega^2-e^{-i(2m-1)\theta})\\&=(\omega^2+1)\prod_{m=1}^{3}[1-2\omega^2\cos(2m-1)\theta+\omega^4]\\&=(1-i\omega)(1+i\omega)\prod_{m=1}^{3}[(1-\omega^2)+2i\omega\cos m\theta]\\&\qquad[(1-\omega^2)-2i\omega\cos m\theta]\\&=\lim_{\sigma\to 0}(1+p^*)(1+p)\prod_{m=1}^{3}[(1+p^2)+2p\cos m\theta]\\&\qquad\times[(1+p^{*2})+2p^*\cos m\theta],\end{aligned}$$

where $\theta=\pi/7$, the seventh roots of unity have been obtained from De Moivre's theorem, simple trigonometric manipulations have been omitted, and, in the final step, p has been substituted for $i\omega$ and p^*, its complex conjugate, for $-i\omega$. By inspection, we may now write

$$\begin{aligned}S(p)=[&(1+p)(1+2p\cos\theta+p^2)\\&\times(1+2p\cos 2\theta+p^2)(1+2p\cos 3\theta+p^2)]^{-1},\end{aligned}$$

and, if we let $d_m=2\cos m\theta=2\cos(\pi m/7)$, the result given in the body of the paper is obtained.

APPENDIX II

We wish to calculate the transient response of a seventh-order Butterworth filter to a unit step function of voltage applied at the input at $t=0$. The resulting output[6] is the inverse Laplace transform of $S(p)/p$, which can be written from Appendix I as

$$S(p)/p=[\prod_{m=0}^{3}(p-p_m^+)(p-p_m^-)]^{-1},$$

where $p_0^+=0$, $p_0^-=-1$, and for $m>0$ $p_m^{\pm}=-e^{\mp im\theta}$, with $\theta=\pi/7$.

The inverse Laplace transform $A(t)$ of $S(p)/p$ is found to be

$$\begin{aligned}A(t)=1-e^{-t}&[\prod_{m=1}^{3}(1+p_m^+)(1+p_m^-)]^{-1}\\&+\exp(p_1^+t)[(p_1^+-p_1^-)\prod_{m=0,2,3}(p_1^+-p_m^+)(p_1^+-p_m^-)]^{-1}\\&+\exp(p_1^-t)[(p_1^--p_1^+)\prod_{m=0,2,3}(p_1^--p_m^+)(p_1^--p_m^-)]^{-1}\\&+\exp(p_2^+t)[(p_2^+-p_2^-)\prod_{m=0,1,3}(p_2^+-p_m^+)(p_2^+-p_m^-)]^{-1}\\&+\exp(p_2^-t)[(p_2^--p_2^+)\prod_{m=0,1,3}(p_2^--p_m^+)(p_2^--p_m^-)]^{-1}\\&+\exp(p_3^+t)[(p_3^+-p_3^-)\prod_{m=0}^{2}(p_3^+-p_m^+)(p_3^+-p_m^-)]^{-1}\\&+\exp(p_3^-t)[(p_3^--p_3^+)\prod_{m=0}^{2}(p_3^--p_m^+)(p_3^--p_m^-)]^{-1}.\end{aligned}$$

Since p_m^- is the complex conjugate on p_m^+ and vice versa for $m>0$, the third and fourth, fifth and sixth, and seventh and eighth, terms are complex conjugates. The above result can, after considerable manipulation, be simplified to

$$\begin{aligned}A(t)=1-e^{-t}&[64\alpha_2^2\alpha_3^2\beta_1^2]^{-1}-e^{-\alpha_1 t}\sin\beta_1 t[32\alpha_2\alpha_3^2\beta_1^2\beta_2]^{-1}\\&+e^{-\alpha_2 t}\cos\beta_2 t[32\alpha_1\alpha_2\alpha_3^2\beta_1\beta_2]^{-1}+e^{-\alpha_3 t}\sin\beta_3 t\\&\times[32\alpha_1\alpha_2\alpha_3\beta_1\beta_2\beta_3]^{-1},\end{aligned}$$

where $\alpha_m=d_m/2=\cos m\theta$, $\beta_m=\sin m\theta$. If we now abandon the restriction $\omega_0=1$, let $t\to\omega_0 t=\tau$, and evaluate the terms, we obtain

$$\begin{aligned}A(\tau)=1&-4.31204e^{-\tau}-6.87748e^{-0.900968\tau}\sin(0.433884\tau)\\&+3.31204e^{-0.623489\tau}\cos(0.781833\tau)\\&+0.755938e^{-0.222519\tau}\sin(0.974929\tau),\end{aligned}$$

where the numbers are expected to be correct to at least four decimal places. A similar but less accurate result given by Wallman was discovered already worked out by a different method[7] after the above work was

[6] J. R. Macdonald and M. K. Brachman, Revs. Modern Phys. 28, 393–422 (1956).

[7] G. E. Valley, Jr., and H. Wallman, *Vacuum Tube Amplifiers* (McGraw-Hill Book Company, Inc., New York, 1948), pp. 282–284.

completed. Wallman's result contains a very small term involving $\sin(0.781833\tau)$ for which there is no theoretical justification. It arises because he calculated the impulse response $B(\tau)$ and obtained $A(\tau)$ from it by integration. $B(\tau)$ may be calculated from the present value of $A(\tau)$ by differentiation, using

$$B(\tau)=A(0)\delta(\tau)+\frac{dA(\tau)}{d\tau}.$$

The result obtained is in good agreement with Wallman's expression.

A test of the accuracy of the present value is given by the relations $A(0)=B(0)=0$ which theoretically hold for the present situation. The numerical expression for $A(\tau)$ gives exactly $A(0)=0$ and one finds that it leads to $B(0)=-2\times10^{-5}$, confirming that the result for $A(\tau)$ is correct to at least four decimal places.

THE JOURNAL OF THE ACOUSTICAL SOCIETY OF AMERICA VOLUME 29, NUMBER 12 DECEMBER, 1957

Laboratory Standard Ceramic Microphone

WILLIAM NEWITT
Electro-Voice, Inc., Buchanan, Michigan
(Received July 26, 1957)

Microphones using barium titanate disk ceramics in conjunction with a split-tube diaphragm have been designed and constructed. Frequency response measurements were obtained by use of reciprocity techniques and by comparison with a known standard.

Sensitivities from −86 to −88 db referred to one volt per dyne per square centimeter, were obtained with a frequency response of plus or minus one db from 10 cycles to 30 kilocycles. The rugged construction and high stiffness of the microphone make it adaptable for use in high sound pressures, and for sound measurement in liquids.

The paper discusses theoretical relations pertinent to the development, describes the construction, and presents performance data of the microphone and associated electronic equipment.

IN the selection of a standard laboratory microphone, small size was desirable as well as features which would permit use of the microphone in media where static pressures greater than one atmosphere may be encountered. Also, it was desirable to have the microphone fairly rugged. The output level of the microphone need not be high, but the threshold sensitivity (minimum detectable sound pressure) must be as low as possible. It was desirable to have a microphone which was usable from 20 cycles up to well within the ultrasonic range, although the response need not be absolutely "flat" within this range.

Two basic types of generating systems were considered, the velocity type and the displacement type. Velocity systems, of which the popular dynamic microphone is representative, produce voltages which depend on the velocity of the diaphragm or member which is exposed to the sound pressure being measured. The velocity of the diaphragm will then be proportional to the force which actuates it, or the pressure imposed upon it, and inversely proportional to the mechanical impedance of the diaphragm. If the applied pressure varies sinusoidally, as is the case for sound pressure, one will find that the magnitude of the diaphragm velocity, hence the rms voltage output, will vary with frequency if the mechanical impedance varies. Since the velocity microphone diaphragm generally has mass, compliance, and resistance, one can expect a mechanical impedance, and therefore output voltage, which will vary with frequency in some manner. In an effort to keep the frequency response of velocity devices constant and output level high, masses have been made smaller, and compliances have been made larger, so that the mechanical impedance of the diaphragm will approach a pure resistive condition, without changing the diaphragm resonance frequency or mechanical resistance.

The resultant high compliance of the velocity device, however, is not a most desirable factor where high static pressures are expected, for the static excursion of the diaphragm may carry it into a nonlinear region, and produce distortion in the sound-pressure voltage output. Some sort of pressure equalization device would be needed to approach the fulfillment of the requirements described at the beginning of this article.

The frequency range of operation of velocity devices employing diaphragms must extend upward from the fundamental resonant frequency of the diaphragm. Below this point, the diaphragm mechanical compliance (taking into account the acoustical compliance associated with the diaphragm) eventually becomes the determining factor in the mechanical impedance, thus resulting in a voltage output which drops as the frequency is decreased. Above the resonant frequency, the mass associated with the diaphragm becomes predominant; however, a considerable amount of this mass is contributed by the acoustical load on the diaphragm, which becomes more resistive as the frequency is